

ESR characterization of Fe(III) ions in polycrystalline cation-deficient FeAl₂O₄ spinel

B. GILLOT

Laboratoire de Recherches sur la Réactivité des Solides, Faculté des Sciences Mirande, B.P. 138 21004 Dijon Cedex, France

B. CHAILLOT

Laboratoire de Chimie Analytique, UER des Sciences Pharmaceutiques et Biologiques, Faculté de Médecine et de Pharmacie, Boulevard Jeanne d'Arc, 21033 Dijon Cedex, France

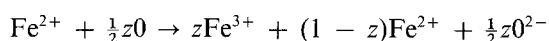
Polycrystalline samples of cation-deficient FeAl₂O₄ spinel with Fe³⁺ ions and vacancies on both octahedral and tetrahedral sites have been investigated by electron spin resonance (ESR). For samples annealing at 1100° C and slightly oxidized (≤ 0.16 wt% Fe³⁺), the ESR spectrum originates from Fe³⁺ ions located in trigonally distorted octahedral sites of α -Al₂O₃ formed during the annealing and also from Fe³⁺ ions introduced by oxidation at low temperature in octahedral sites of spinel structure. The samples with concentration between 0.16 and 1.6 wt% Fe³⁺ show the majority of Fe³⁺ ions to be on tetrahedral sites and the rhombic symmetry around the Fe³⁺ ions is attributed to the presence of cation vacancies.

1. Introduction

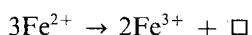
Within the setting of our work on particular properties that some finely-divided spinels containing iron(II) have to oxidize to γ -cation deficient spinels [1], we propose to obtain by electron spin resonance (ESR) spectroscopy, supplementary information on the environment of the Fe³⁺ ions introduced in small amount by oxidation and annealing in the FeAl₂O₄ spinel lattice. In this spinel, at room or liquid nitrogen temperatures only Fe³⁺ (a 3d⁵ ion) can be detected by ESR, whereas Fe²⁺ (a d⁶ ion) can be seen only at liquid helium temperature, because of its short relaxation time [2]. Since Fe³⁺ ions have zero orbital angular momentum in the free atom, the resonance should arise from the amount of Fe³⁺ ion in iron(II) aluminate. Any changes in the electric fields of the neighbouring ions of Fe³⁺ ions should distort the orbit of the 3d electrons and should provide valuable information about the crystal electric field variation.

2. Samples and measurements

Details of FeAl₂O₄ preparation via a metal-organic precursor have been reported previously [3]. The Fe³⁺ ions are generated by low temperature oxidation (between 160 and 300° C) in the following way: Fe²⁺ are replaced by Fe³⁺ and cation vacancies according to the formula

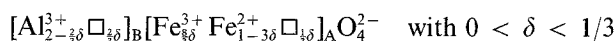


with



where \square is the vacant site and z the oxidation parameter. Crystallographic and magnetic studies [4] have shown that the vacancies are distributed $\frac{1}{3}$ on tetrahedral sites (A sites) and $\frac{2}{3}$ on octahedral sites (B

sites). Thus, for partial oxidation, the ion distribution in the spinel lattice is given by the formula



In this way we can study the change in the ESR spectrum as a function of the increasing number of Fe³⁺ ions present on A sites. The different oxidation ratios were obtained by means of a Setaram microbalance with a sensitivity of 10⁻³ mg by establishing the ratio of weight gain corresponding to the partial oxidation expected to the full oxidation of Fe²⁺ ions. The values selected for this study are $\delta = 10^{-3}$, $\delta = 5 \times 10^{-3}$ (for samples oxidized at 160° C), $\delta = 2.5 \times 10^{-2}$, $\delta = 5 \times 10^{-2}$ (for samples oxidized at 290° C) which corresponds to a concentration range of 0.032 to 1.60 wt% Fe³⁺. As the purpose of the present investigation is not the study of the ferromagnetic resonance of the ferrite, but rather the use of ESR to obtain information on coordination of Fe³⁺ ions, only γ -cation deficient spinels of low Fe³⁺ content have been prepared.

Previously, in a series of annealing samples at various temperatures (900 and 1100° C) and comparatively to samples prepared at 700° C in which the totality of Fe²⁺ ions reside on A sites [4], it was found that a very small amount of Al³⁺ ions are located at the A sites causing the presence of equal amounts of Fe²⁺ ions on B sites. For sample annealing at 1100° C the inversion degree defined by the parameter λ of the formula $(\text{Fe}_{1-2\lambda}^{2+}\text{Al}_{2\lambda}^{3+})_{\text{A}}(\text{Al}_{2-2\lambda}^{3+}\text{Fe}_{2\lambda}^{2+})_{\text{B}}\text{O}_4^{2-}$ is about 0.01. As the availability for oxidation of Fe²⁺ ions at A sites is much less than that at B sites [5], the oxidation of Fe²⁺ ions on A sites can be avoided if the oxidation temperature was sufficiently low, thus producing Fe³⁺ ions only on the octahedral sublattice. This can be realized if samples were oxidized below

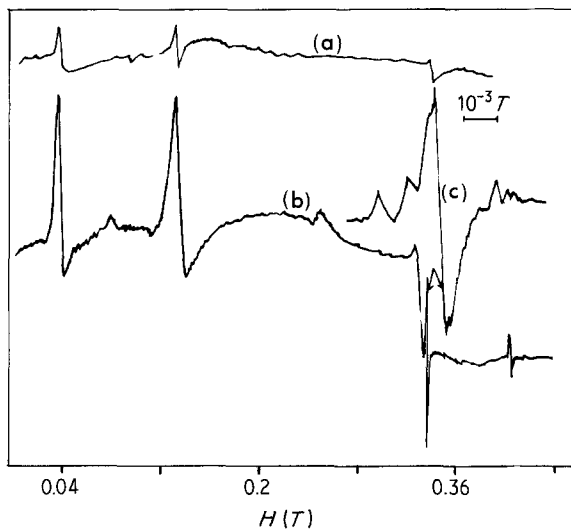


Figure 1 ESR spectra of FeAl_2O_4 spinel. (a) annealing at 900°C with $0.032\text{ wt } \%$ Fe^{3+} ; (b) annealing at 1100°C with $0.16\text{ wt } \%$ Fe^{3+} ; (c) expanded portion of curve (b).

170°C when $\delta = 10^{-3}$ and $\delta = 5 \times 10^{-3}$ values represent approximately the oxidation content of Fe^{2+} ions on B sites.

A portion of oxidized sample (50 mg) was enclosed in a silica ampoule, with a standard ESR tube as a side arm, connected to the vacuum system. After outgassing at room temperature for 1 h (10^{-5} Pa), the powder was transferred to the ESR tube for measurement. The ESR spectra were recorded at room temperature or occasionally at 77 K, using a E-12 Varian spectrometer operating in the X-band (9.52 GHz); the magnetic field was modulated for sensitivity and detection reasons at 100 kHz. The g values have been obtained by comparison with polycrystalline DPPH.

3. Results

First-derivate X-band ESR spectra at room temperature for iron aluminate spinels annealing at 900 and 1100°C with 0.032 and $0.16\text{ wt } \%$ Fe^{3+} are depicted in Fig. 1. Apparent g values and peak-to-peak line widths of ESR signals are listed in Table I. Both samples give a complex multiline spectrum with two sharp absorptions at low field ($H \approx 0.04\text{ T}$ and $H \approx 0.136\text{ T}$) and depending on the annealing temperature one or two signals on the high-field side. At 0.337 T there is a very sharp symmetrical signal of $6 \times 10^{-4}\text{ T}$ linewidth (Fig. 1, curve c) and a broad

TABLE I Room temperature ESR characteristics of Fe^{3+} ions in FeAl_2O_4 . Only the more intense signals are given

$\delta = 0.005$ Sample annealing at 1100°C							
g_{eff}	16.7	—	4.90	—	—	2.04	2.001
Linewidth	50	—	100	—	—	110	6
$\Delta H(10^{-4}\text{ T})$							
$\delta = 0.025$ Sample annealing at 900°C							
g_{eff}	16.3	6.15	—	4.25	—	2.08	—
Linewidth	80	180	—	210	—	160	—
$\Delta H(10^{-4}\text{ T})$							
$\delta = 0.05$ Sample annealing at 900°C							
g_{eff}	16.4	6.11	—	4.26	4.06	2.04	—
Linewidth	90	250	—	50	55	100	—
$\Delta H(10^{-4}\text{ T})$							

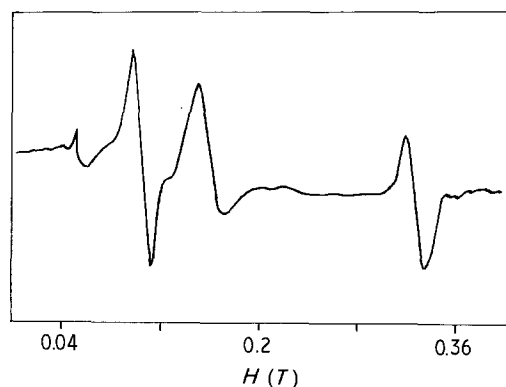


Figure 2 ESR spectra of FeAl_2O_4 spinel annealing at 900°C with $0.8\text{ wt } \%$ Fe^{3+} .

resonance of width 0.01 T centred at about 0.332 T . However, for sample annealing at 900°C (Fig. 1a, curve a) intensities of resonance line are very substantially diminished and sample annealing at 1100°C (Fig. 1, curve b) had additional ESR lines at approximately $810, 0881, 0.0255$ and 0.4100 T .

With increasing Fe^{3+} content (Fig. 2) aluminate spinel annealing at 900°C had ESR features somewhat different than that of the preceding ones in that there are two strong resonances at about 0.107 and 0.16 T with apparent g values being 6.15 and 4.25 , respectively. Furthermore, the resonance at $\approx 0.04\text{ T}$ is also observed. ESR characteristics are given in Table I. The ESR spectrum of sample annealing at 900°C with $1.60\text{ wt } \%$ Fe^{3+} (Fig. 3) differs significantly from the previous one in that the $g = 6.15$ resonance was more intense while the $g = 4.25$ absorption derivate exhibits a doublet. Other signals at $g = 2.64$ and $g = 2.49$ are also observed. In more concentrated samples ($> 2\text{ wt } \%$ Fe^{3+}) magnetic interactions between neighbours occur, and only one central absorption is observed.

4. Discussion and conclusion

The complete explanation of resonance lines would be given in principle by solving the spin-Hamiltonian which included the paramagnetic ion and its couplings to its neighbours suggesting possible local atomic

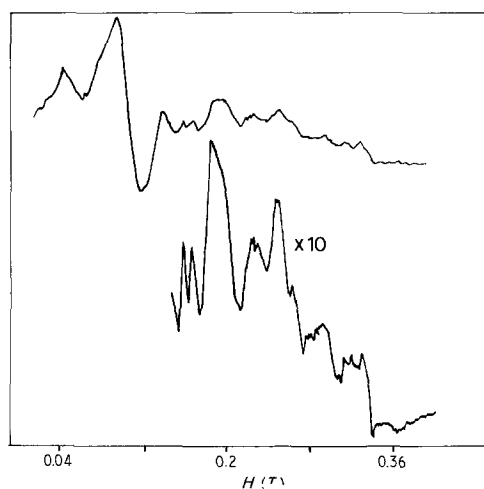


Figure 3 ESR spectra of FeAl_2O_4 spinel annealing at 900°C with $1.6\text{ wt } \%$ Fe^{3+} .

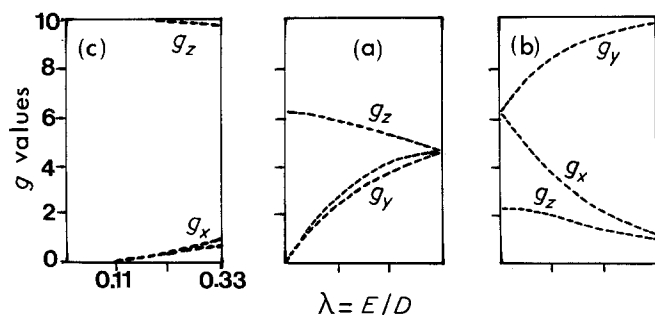


Figure 4 Effective g values for the spin Hamiltonian of Equation 1 plotted against $\lambda = E/D$.

surroundings of the iron. Considering the complexity of spectra owing to the presence of Fe^{3+} ions and vacancies located substitutionally in two crystallographically inequivalent sites of the spinel structure, the interpretation of resonance lines would be made separately.

When the Fe^{3+} concentration in the FeAl_2O_4 spinel is not high (Fig. 1), one can assume that the spectra originate from Fe^{3+} ions located in octahedral sites. The resonance lines with apparent g values of 16.3, 4.9 and 2.08 also have been observed in alumina heated above 1000°C [6, 7] and have been identified as due to Fe^{3+} ions in a trigonally distorted octahedral sites of $\alpha\text{-Al}_2\text{O}_3$. From the conclusions drawn from detailed studies made by Pott and McNicol [6], these features probably correspond to the formation of very small fraction of α -alumina microcrystals containing low Fe^{3+} concentration presumably as a consequence of surface oxidation reaction during the annealing at high temperature in nitrogen. An increase in annealing temperature from 900 to 1100°C shows a better definition and an increase of resonance line intensity associated with increasing Fe^{3+} ions concentration in octahedral sites of $\alpha\text{-Al}_2\text{O}_3$ according to higher degree of inversion in samples annealing at 1100°C . The very sharp symmetrical signal at 0.337T can be attributed to Fe^{3+} ions located on B sites of the spinel lattice. These ions result of the oxidation of Fe^{2+} ions located at B-sites which are more readily oxidized at low temperature than Fe^{2+} ions on A sites. Fig. 1 (curve c) shows an expanded portion in the region of a strong isotropic line with spectroscopic splitting factor g equal to 2.001. Centred upon this line is a set of lines of about one tenth the intensity of the central line. Moreover, the three lines at $g = 8.32$, $g = 2.64$ and $g = 1.64$ arise from Fe^{3+} in an axial or lower symmetry electric field [8]. This indicated that any vacancy necessary for charge compensation must be immediately adjacent to oxygen ion octahedron which surrounds the iron [9]. In seeking an explanation for axial or lower symmetry it appears reasonable to assume that these resonance lines arise from Fe^{3+} ions which have an associated vacancy at one of the 12 nearest-neighbour positions, i.e. in a $[1\ 1\ 0]$ -type direction. We should like to suggest that "trapped holes" may produce a lower symmetry than cubic. If an electron is lost from one of the six oxygen ions in the octahedron surrounding an iron ion vacancy near a trivalent ion, one would have local charge compensation also with this type of centre [8].

With regard to the Fe^{3+} $g = 6.15$ and $g = 4.25$ signals for oxidation content $\delta = 2.5 \times 10^{-2}$ (Fig. 2),

they have been observed together or individually in many powder ESR studies, in particular in glass [10], in titanium compounds [11], in polycrystalline ferrichrome A [12], in haemoglobin [13] or in alumina heated below 900°C [6, 7, 14]. A complete interpretation of g values in the case of a large crystal field splitting of the $S = 5/2$ sextet in Fe^{3+} compared with the Zeeman splitting has been given by Griffith [15] and Castner *et al.* [16] by considering a Hamiltonian of the more general form

$$\mathcal{H} = g\beta HS_z + D[S_z^2 - \frac{1}{3}S(S+1)] + E(S_x^2 - S_y^2) \quad (1)$$

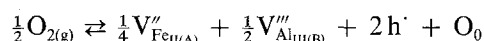
where the first term represents the electronic Zeeman interaction with $g = 2.0023$, D and E are the axial and rhombic field parameters and S_x , S_y , S_z are components of spin along three mutually perpendicular axis x , y and z . The spins experience two couplings S_z^2 and $S_x^2 - S_y^2$ to the neighbouring oxygen ions. Any change in electric field of the Fe^{3+} ions environment will change the D and E constants.

The iron resonance occurring at $g = 6.15$ and $g = 4.25$ can be explained as a function of parameter $\lambda = E/D$ with $0 < \lambda < 1/3$ as proposed by Wickman *et al.* [12] where Fig. 4 represents the variation with λ of the effective g factors for the three crystal field Kramers' doublet considered separately as having effective spin of $\frac{1}{2}$. If $E < D$ the tetragonal arrangement FeO_4 (A sites) with orthorhombic symmetry, give rise to signal at $g = 4.25$ taking the crossing point in the derivative curve (Fig. 4, curve a) which is consistent with $\lambda = \frac{1}{3}$. Therefore at the frequency $\nu = 9.52\text{GHz}$ the parameters are $D > 0.159\text{cm}^{-1}$, $E > 0.053\text{cm}^{-1}$. In the case when E is very much smaller than D (for example $E = 0$), it is the large value of tetragonal field which is responsible for the two resonance lines, the one at $g = 6.15$ (the stronger) and the other at $g = 2$ (Fig. 4, curve b).

From these considerations, we believe that these resonance lines for samples annealing at 900°C with $\lambda \approx 0$ result from Fe^{3+} ions in tetrahedral sites with distortion in their local coordination because of increased accumulation of cation vacancies.

With Kröger and Vinck's notation [17] the formation reaction of cationic vacancies in FeAl_2O_4 at the solid-gas interface may be written considering that one atom of oxygen becomes an O_0 ion on a site of the lattice surface with correlative generation of a metal vacancy due to the diffusion of a cation toward the surface. The balance of matter of the oxidized phase, shows 2Al^{3+} and 1Fe^{2+} missing relative to the spinel structure, therefore, we must consider that the

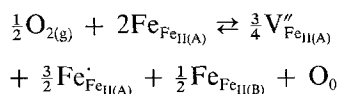
generation of 4O^{2-} is accompanied by three vacancies among which two of Al^{3+} and one of Fe^{2+} . If the vacancies are distributed by $\frac{1}{3}$ on A sites and $\frac{2}{3}$ on B sites as in the case of total oxidation, we may write in considering a total ionization of defects



However, for a slight oxidation content the vacancies may be distributed on the sites on which they are generated, i.e. on tetrahedral sites [18]. We then have



The electron transfer, an ionization process, involves iron vacancies, Fe^{3+} ions and oxygen atoms according to



That is, the electrons are transferred from oxygen into the iron vacancy, V_{FeII}'' with the consequence of reduced charged O_2^{2-} being formed. This implies that the averaged Coulomb and exchange potentials exerted upon paramagnetic Fe^{3+} ion by its environment are changed [19]. For example, if in the nearest neighbouring tetrahedrons the Fe^{2+} ion is replaced by a Fe^{3+} ion, the effective charges on the oxygen ion in the two corners will change and give $S_x^2 - S_y^2$ component to the Hamiltonian or $g = 4.25$ case. A single charge on one corner will give the S_z^2 component and increase the g value or $g = 6.15$ case. As we have remarked, the resonance intensities are oxidation content dependent indicating that the concentration of electrons associated with iron vacancies and Fe^{3+} ions change. The fact that the peak intensity at $g = 6.15$ is increased for sample annealing at 900°C with $\delta = 0.05$ means that the probability for iron ions

of having a single positive charge in the immediate neighbourhood is quite high.

References

1. B. GILLOT and A. ROUSSET, *J. Sol. Stat. Chem.* **65** (1986) 322.
2. J. E. WERTZ, P. AUZINS, J. H. E. GRIFFITHS and J. W. ORTON, *Phys. Rev.* **106** (1957) 66.
3. F. CHASSAGNEUX and A. ROUSSET, *J. Sol. Stat. Chem.* **16** (1976) 161.
4. B. GILLOT, F. BOUTON, F. CHASSAGNEUX and A. ROUSSET, *Mater. Res. Bull.* **15** (1980) 1.
5. B. GILLOT, F. JAMMALI, F. CHASSAGNEUX, C. SALAVAING and A. ROUSSET, *J. Sol. Stat. Chem.* **45** (1982) 317.
6. G. T. POTT and B. D. McNICOL, *Discus. Farad. Soc. Surf. Chem. Oxides* **52** (1971) 121.
7. A. C. VAJPEI, A. ROUSSET, B. MAACHI, M. GOUGEON, N. FAVILLIER and G. ABLART, *J. Mater. Sci. Lett.* **6** (1987) 1167.
8. B. HENDERSON, J. E. WERTZ, T. P. P. HALL and R. D. DOWSING, *J. Phys. C* **4** (1971) 107.
9. R. S. De BIASI and A. CALDAS, *ibid.* **10** (1977) 107.
10. R. H. SANDS, *Phys. Rev.* **99** (1955) 1222.
11. J. A. GAINON, *ibid.* **134** (1965) 1300.
12. H. H. WICKMAN, M. P. KLEIN and D. A. SHIRLEY, *J. Chem. Phys.* **42** (1965) 2113.
13. B. CHAILLOT, Thesis, Dijon University (1984).
14. F. GESMUNDO and C. De ASMUNDIS, *J. Phys. Chem Solids* **35** (1974) 1007.
15. J. S. GRIFFITH, *Proc. R. Soc. A* **235** (1956) 23.
16. T. CASTNER, G. S. NEWELL, W. C. HOLTON and C. P. SLICHTER, *J. Chem. Phys.* **32** (1960) 668.
17. F. A. KROGER and H. J. VINCK, in "Solid State Physics", edited by F. Seitz and D. Turnbull (Academic Press, New York, 1956) p. 307.
18. B. GILLOT and P. BARRET, *C. R. Acad. Sc. Paris* **C278** (1974) 1477.
19. T. NOWOK and V. I. STENBERG, *Appl. Surf. Sci.* **29** (1987) 463.

Received 29 February
and accepted 8 July 1988